JACS
JOURNAL OF THE AMERICAN CHEMICAL SOCIETY

Communication

pubs.acs.org/JACS

Controlled pH Stability and Adjustable Cellular Uptake of Mixed-Charge Nanoparticles

Pramod P. Pillai, Sabil Huda, Bartlomiej Kowalczyk,* and Bartosz A. Grzybowski*

Department of Chemistry and Department of Chemical Engineering, Northwestern University, 2145 Sheridan Road, Evanston, Illinois 60208, United States

Supporting Information

ABSTRACT: Nanoparticles functionalized with mixed self-assembled monolayers (m-SAMs) comprising positively and negatively charged thiols are stable at both low and high pH but precipitate sharply at the pH where the charges on the particle are balanced (pH^{prec}). By adjusting the proportion of the positively and negatively charged ligands in the m-SAM or changing particle size, pH^{prec} can be varied flexibly between ~4 and ~7. In addition, changes in the SAMs' composition and particles' net charge translate into different degrees of cellular uptake. Remarkably, the presence of the positively charged thiols allows for the uptake of particles having net negative charge.

Nanoparticles (NPs) functionalized with charged organic ligands exhibit a range of unique properties both in solution and in the solid state. In solution, such "nanoionic" particles[1−3] precipitate upon temperature increase,[4] have pK_a values that depend on the particle size/curvature,[5] and can crystallize into open-lattice crystals.[6,7] In the solid state, their thin films can trap electrons in polaronic states, giving rise to phenomena such as inverse photoconductance.[8] While we have previously studied rather exhaustively the properties of NPs covered with one type of charged functionality,[1−10] much less is known[11−13] about the properties of NPs covered with mixed self-assembled monolayers (m-SAMs) comprising both positively and negatively charged ligands (Figure 1a). As we show here, such mixed-charge (MC) NPs combine three unique properties: (1) They are soluble at both low and high pH and precipitate only around the pH value corresponding to the neutralization of the surface charge (pH^{prec}). (2) The value of pH^{prec} can be varied flexibly over several pH units[14] by adjusting the m-SAM composition and/or NP size. In this way, our MC NPs can be made compatible with physiological pHs and buffer solutions. (3) Remarkably, varying the net charge on the NPs changes their propensity to penetrate into mammalian cells. In particular, the presence of the positively charged thiols on the NPs allows for the uptake of particles having net negative charge, which is typically difficult to achieve, especially for NPs with diameters of a few nanometers.[15,16]

Precursor gold NPs (AuNPs) stabilized with dodecylamine (DDA) and having sizes of 4.2 ± 0.5, 5.2 ± 0.5, 8.0 ± 0.5, 9.5 ± 0.8, and 11.5 ± 0.8 nm were prepared as described previously[1,2] [see section 1 in the Supporting Information (SI)]. These NPs were then functionalized with m-SAMs comprising neutral 11-mercaptoundecanoic acid (MUA) and positively charged *N,N,N*-trimethyl(11-mercaptoundecyl)ammonium ion (TMA) (Figure 1a). This was done by soaking the DDA AuNPs (0.15 mM in terms of Au atoms) for at least 15 h in toluene/CH_2Cl_2 mixtures containing MUA and TMACl in various proportions

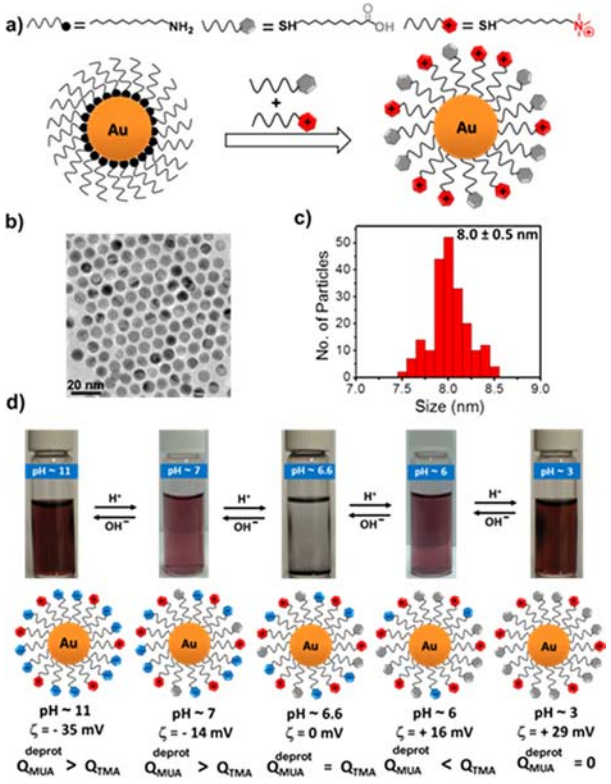

Figure 1. Preparation and stability of mixed-charge AuNPs. (a) Scheme of a place-exchange reaction between DDA-functionalized AuNPs and a mixture of MUA and TMA thiols. (b) Representative TEM image of 8.0 ± 0.5 nm MC AuNPs. (c) Corresponding size distribution based on TEM statistics for >200 NPs (see Figure S2). (d) Images of vials containing 8.0 nm MC NPs (covered with an m-SAM with α_{surf} = 2.5) at various pH. The particles are stable in solution except around pH^{prec} = 6.6. The schemes below the images illustrate the charge on the m-SAMs[17] (blue = negative/deprotonated MUA, gray = neutral/protonated MUA, red = positive TMA). pH^{prec} is the pH where the charges on the NP are balanced ($Q_{MUA}^{deprot} + Q_{TMA} = 0$).

Received: January 5, 2013
Published: March 26, 2013

   dx.doi.org/10.1021/ja4001272 | *J. Am. Chem. Soc.* 2013, 135, 6392−6395

($\alpha_{soln} = c_{soln}^{MUA}/c_{soln}^{TMA}$ = 2, 3, and 9). In all of the experiments, the total concentration of thiol was kept constant and was in ~40-fold excess relative to the number of surface sites on the NPs. After ligand exchange, the unbound thiols were removed by precipitating the NPs and washing the precipitate multiple times with copious amounts of CH_2Cl_2. The purified NPs were then redissolved in water, and the pH of all solutions was adjusted to ~11 using tetramethylammonium hydroxide. Under these conditions, the MUA ligands were fully deprotonated, resulting in MC NPs. The exact compositions of the two ligands in the on-particle m-SAMs were determined by ^{1}H NMR experiments to be $\alpha_{surf} = c_{surf}^{MUA}/c_{surf}^{TMA}$ = 1.6, 2.5, and 7.7 (see the SI).

The stability of the MC NPs (illustrated in Figure 1d) was studied in a series of titrations (see the SI) monitored by UV–vis spectroscopy and ζ-potential measurements (Figure 2). For

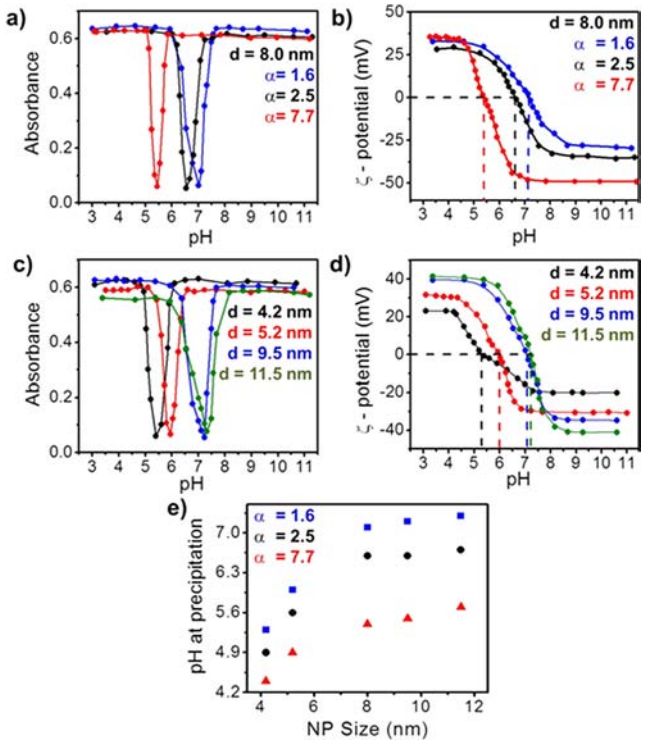

Figure 2. Variation of pH^{prec} with m-SAM composition and NP size. (a) Plots of the intensity of the AuNP surface plasmon resonance (SPR) peak (here, at 520 nm for 8.0 ± 0.5 nm MC NPs) as a function of pH for different m-SAM compositions [α_{surf} = 1.6 (blue), 2.5 (black), 7.7 (red)]. At pH^{prec}, the intensity of the SPR band is minimal because of NP precipitation. (b) Corresponding plots of the ζ potential; at pH^{prec}, ζ = 0. (c, d) Data analogous to those in (a) and (b) but for NPs with different sizes but the same surface composition (α_{surf} = 1.6). (e) Plot summarizing the values of pH^{prec} for all of the experiments (for the raw data, see Figures S4 and S5).

all NP sizes and m-SAM compositions, the particles were stable at both low and high pH. At low pH, the MUA ligands were protonated, and the NPs had net positive charge (ζ potential > 0) due to the TMA groups; such like-charged particles were stabilized in solution by electrostatic repulsions.[2−4] Conversely, at high pH, where MUA was deprotonated, the negative charge of these ligands (Q_{MUA}^{deprot}) was greater in magnitude than the positive charge of the TMA ligands (Q_{TMA}), affording NPs with a net negative charge (ζ potential < 0) that again were stabilized in solution by like-charge repulsions. Between these two pH regimes, the NPs precipitated when the surface charge on the NPs was neutralized (i.e., $Q_{MUA}^{deprot} + Q_{TMA} = 0$) and the ζ potential was equal to zero. In the absence of electrostatic repulsions, the NPs aggregated because of the van der Waals attractions between NP cores[18] and hydrogen bonding between partially protonated MUA ligands. Importantly, the pH value corresponding to NP precipitation, pH^{prec}, depended on the composition of the m-SAM and/or on the size of the NPs, as summarized in Figure 2e (for the raw data, see Figures S4 and S5 in the SI) and discussed below.

(i) Effect of m-SAM composition. For a given NP size, pH^{prec} decreases as the proportion of MUA increases (progression from blue markers for α_{surf} = 1.6 through black markers for α_{surf} = 2.5 to red markers for α_{surf} = 7.7; Figure 2a,b,e). The magnitude of the change in pH^{prec} is ~1 pH unit for smaller NPs and almost 2 pH units for larger particles. pH^{prec} decreases with increasing α_{surf} because there are more −COOH groups present on the NP, so a smaller fraction of these groups needs to be deprotonated (i.e., a lower pH is needed) to achieve electroneutrality of the surface-bound ligands (i.e., $Q_{MUA}^{deprot} + Q_{TMA} = 0$, where $Q_{MUA}^{deprot} + Q_{MUA}^{prot} = Q_{MUA}^{total}$). For a discussion of how the pK_a of the MUA ligands changes with the NP surface composition, see section 2 in the SI.

(ii) Effect of NP size. For a given m-SAM composition, pH^{prec} increases with increasing NP diameter (Figure 2c,d,e). Over the range of NP sizes studied, the magnitude of this increase is ~2 pH units (e.g., for α_{surf} = 1.6, pH^{prec} = 5.3 for 4.2 nm NPs and pH^{prec} = 7.3 for 11.5 nm NPs). Again, this trend can be explained on the basis of the proximity of the carboxylic groups:[5,19] For a given value of α_{surf}, as the NP size increases (and the NP curvature decreases), the average distance between the COOH groups of the MUA ligands decreases. Consequently, the deprotonated ligands experience stronger electrostatic repulsions. The SAM responds to this energetically unfavorable situation by "regulating"[5,19] the ligands' charges by shifting the acid–base equilibrium toward the protonated state. As a result, at a given solution pH, the fraction of charged MUA ligands decreases as the NPs become larger. For our MC NPs, this means that a higher pH is needed to deprotonate enough MUAs to compensate for the positive charges of the TMA ligands and cause NP precipitation. As expected, the increase in pH^{prec} levels off when the NPs become large and increasingly "flat" on the scale of the m-SAM thickness. As this happens, the average distance between head groups, d, tends to the value d_0 ≈ 0.463 nm (corresponding to the packing of thiolates on a flat gold surface[20]), since $d(R) \approx d_0(R + L)/R$, where R is the radius of the NP metal core and L is the SAM thickness (here ~1.5 nm).[6] The incremental change in d with changing R then levels off at large R, as $dd/dR \sim 1/R^2$.

In the context of their potential biological applications, an important property is that MC NPs are stable in gels and biologically relevant buffers such as phosphate-buffered saline (see section 3 in the SI) as well as cell-culture media. In particular, this last property enables what is perhaps the most important result of this study, namely, the ability to control the degree of uptake of MC NPs into mammalian cells. Figure 3 summarizes the results of experiments in which 5.2 and 9.5 nm MC NPs with relative net charge (Q^{net}) varying from fully negative to fully positive were added to the culture of mammalian cells (here, Rat2 fibroblasts). After incubation for 24 h, the cell viability was assessed by confocal microscopy using fluorescent dyes (LIVE/DEAD Viability/Cytotoxicity Kit, Invitrogen). The green color of the cells in Figure 3a shows that

dx.doi.org/10.1021/ja4001272 | J. Am. Chem. Soc. 2013, 135, 6392−6395

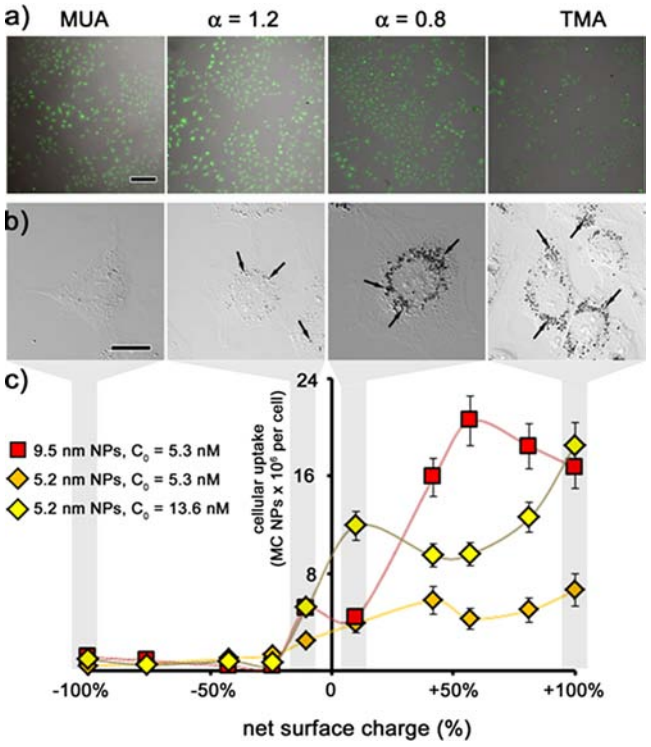

Figure 3. Cell viability and uptake studies for MC NPs with different sizes and surface compositions. (a) Confocal images of Rat 2 cells after incubation for 24 h in the presence of 2.5 mM (in terms of metal atoms, 13.6 nM in terms of NPs) solution of 5.2 nm MC NPs. Cells were stained with calcein AM and ethidium homodimer-1. The observation of only green fluorescence indicates that all of the cells are alive. Scale bar = 100 μm and is the same for all images. (b) Optical images of Rat 2 cells illustrating different degrees of MC NP uptake (indicated by arrows; for higher resolution images, see section 5 in the SI). Uptaken NPs (for $\alpha_{surf} \gtrsim 1.2$) are localized in the cytoplasm but not in the nuclei, in agreement with previous studies[21] reporting nuclear uptake for 2.2 nm NPs but not 4 nm NPs. Scale bar = 25 μm. (c) ICP data quantifying the degree of cellular uptake as a function of relative net charge (Q^{net}) on the MC NPs. Q^{net} is related to the surface composition by the equation $Q^{net} = (\chi_{TMA} - \chi_{MUA})\cdot 100\%$, where the χ's are the mole fractions of the thiols on the NP (assuming that all MUA groups are deprotonated in experimental conditions). Error bars correspond to standard deviations based on at least three ICP experiments for each set of conditions.

none of the MC NPs were cytotoxic at the low concentrations used in these studies.[22]

At the same time, the NPs were uptaken by the cells, and the degree of their internalization varied with the NP charge. This was quantified by the inductively coupled plasma (ICP) method (see section 1 in the SI for experimental details), as shown in Figure 3c. Two general trends were observed: (*i*) at the same concentration, large NPs are internalized more readily than small ones; and (*ii*) for NPs of a given size, cellular uptake increases with NP concentration. These observations agree with previous studies[23] also in terms of the degree of uptake (2−20 × 10^6 MC NPs per cell here vs 1−15 × 10^6 NPs per cell for DNA-coated NPs at comparable concentrations of 5−15 nM in ref 23).

The new feature of our MC NPs is that the degree of uptake depends on the net particle charge. Although the highest uptake for the 5.2 nm NPs was observed for particles fully coated with TMA, the uptake remained appreciable even for MC NPs having small but negative net charge ($\chi_{MUA} \approx 0.55$, $\alpha_{surf} = 1.2$). For the 9.5 nm NPs, the maximal uptake was observed for $\chi_{MUA} \approx 0.21$ ($\alpha_{surf} = 0.27$). Also in this case, NPs having a small negative net charge were uptaken.

It is instructive to put these findings in the context of a canonical view of cellular uptake[24−28] of NPs. It is generally accepted that the initial step of this process is mediated by electrostatic interactions between the negatively charged phospholipids in the cell membrane and the ligands on the NP. Only upon binding of the NPs to the cell's surface receptors does the local decrease in Gibbs free energy[27] enable the membrane to wrap around the NP and internalize it into an endosome (note that endosomes localize in the cytoplasm or, depending on the NP size, shape, and surface functionalization, in different organelles; see ref 21). In line with this picture, numerous previous studies have shown that positively charged NPs are internalized more easily than neutral particles.[15,16] At the other extreme, negatively charged NPs are typically not uptaken *unless* their SAM "corona" is modified with extracellular serum proteins,[25,28,29] as in Mirkin's antisense-oligonucleotide-functionalized NPs (ASNPs).[23]

In our system, the positively charged thiols "mask" the electrostatic repulsion between the membrane and the m-SAM's negatively charged component. This enables uptake of NPs with charges ranging from highly positive through almost neutral to slightly negative. This ability to achieve cellular uptake over a wide range of charge is significant in light of in vivo studies showing that although highly positive NPs are uptaken most readily, they also have several untoward effects, including hemolysis and platelet aggregation.[24] The fact that charge effects are similar for NPs of different sizes is also important, since by varying both the NP size and the surface composition one can aim for an optimal balance between cellular uptake rates and circulation times,[30] which depend on the degree of opsonization and recognition by the mononuclear phagocyte system.

In summary, immobilization of oppositely charged MUA and TMA ligands onto NPs gives rise to a class of nanoions[1−4,6,7] that exhibit unique stability at low and high pH, sharp precipitation at a pH corresponding to the neutralization of the surface charge, and a degree of cellular uptake controlled by the net charge. While the controllable cellular uptake is probably the most immediately relevant application, we envision one more intriguing avenue for future research: the ability to adjust the precipitation point of the MC NPs could be used for pH-specific biological targeting, especially of tumors, whose extracellular pH (pH_e) of ∼6.5 is lower by about one unit than the pH of the surrounding healthy tissue (under physiological conditions, $pH_e \approx 7.4$).[31−33]

■ ASSOCIATED CONTENT

Ⓢ Supporting Information

^{1}H NMR spectra of MUA and TMA ligands ($\alpha_{surf} = 1.6$) in DMSO-d_6 after etching of the AuNP cores, TEM images and size distributions of MC NPs, experiments on the stability of MC NPs, high-resolution images of MC NP uptake, and detailed descriptions of experimental procedures. This material is available free of charge via the Internet at http://pubs.acs.org.

■ AUTHOR INFORMATION

Corresponding Author

b-kowalczyk@northwestern.edu; grzybor@northwestern.edu

Notes

The authors declare no competing financial interest.

■ ACKNOWLEDGMENTS

This work was supported by the Nonequilibrium Energy Research Center, an Energy Frontier Research Center funded by the U.S. Department of Energy, Office of Science, Office of Basic Energy Sciences under Award DESC0000989. The authors would like to thank Ms. Jiwon Kim and Dr. Ahmet F. Demirörs for their help with ICP measurements.

■ REFERENCES

(1) Kalsin, A. M.; Kowalczyk, B.; Wesson, P.; Paszewski, M.; Grzybowski, B. A. *J. Am. Chem. Soc.* **2007**, *129*, 6664.
(2) Kalsin, A. M.; Kowalczyk, B.; Smoukov, S. K.; Klajn, R.; Grzybowski, B. A. *J. Am. Chem. Soc.* **2006**, *128*, 15046.
(3) Bishop, K. J. M.; Grzybowski, B. A. *ChemPhysChem* **2007**, *8*, 2171.
(4) Bishop, K. J. M.; Kowalczyk, B.; Grzybowski, B. A. *J. Phys. Chem. B* **2009**, *113*, 1413.
(5) Wang, D. W.; Nap, R. J.; Lagzi, I.; Kowalczyk, B.; Han, S. B.; Grzybowski, B. A.; Szleifer, I. *J. Am. Chem. Soc.* **2011**, *133*, 2192.
(6) Kalsin, A. M.; Fialkowski, M.; Paszewski, M.; Smoukov, S. K.; Bishop, K. J. M.; Grzybowski, B. A. *Science* **2006**, *312*, 420.
(7) Kowalczyk, B.; Kalsin, A. M.; Orlik, R.; Bishop, K. J. M.; Patashinskii, A. Z.; Mitus, A.; Grzybowski, B. A. *Chem.—Eur. J.* **2009**, *15*, 2032.
(8) Nakanishi, H.; Bishop, K. J. M.; Kowalczyk, B.; Nitzan, A.; Weiss, E. A.; Tretiakov, K. V.; Apodaca, M. M.; Klajn, R.; Stoddart, J. F.; Grzybowski, B. A. *Nature* **2009**, *460*, 371.
(9) Nakanishi, H.; Walker, D. A.; Bishop, K. J. M.; Wesson, P. J.; Yan, Y.; Soh, S.; Swaminathan, S.; Grzybowski, B. A. *Nat. Nanotechnol.* **2011**, *6*, 740.
(10) Walker, D. A.; Wilmer, C. E.; Kowalczyk, B.; Bishop, K. J. M.; Grzybowski, B. A. *Nano Lett.* **2010**, *10*, 2275.
(11) Liu, X. S.; Jin, Q.; Ji, Y.; Ji, J. *J. Mater. Chem.* **2012**, *22*, 1916.
(12) Liu, X. S.; Huang, H. Y.; Jin, Q.; Ji, J. *Langmuir* **2011**, *27*, 5242.
(13) Bonitatibus, P. J.; Torres, A. S.; Kandapallil, B.; Lee, B. D.; Goddard, G. D.; Colborn, R. E.; Marino, M. E. *ACS Nano* **2012**, *6*, 6650.
(14) We note that when both positive and negative charges are present on the same zwitterionic ligand, the ratio of positive and negative charges on the NP is fixed and cannot be modified as in our system. With such zwitterionic ligands, the two groups do not contribute equally to the overall properties and surface charge of the NP because the charge of the group that is buried deeper in the monolayer is screened by the opposite-polarity functionality closer to the NP surface; it is the latter functionality that is exposed to the environment and has a more pronounced influence on the NP's properties. In a recent attempt, Liu et al.[12] synthesized zwitterionic NPs functionalized with two oppositely charged thiols (bearing cationic quaternary ammonium and anionic sulfonate groups). However, these NPs had pH-independent solubility and were stable over the entire pH range because both kinds of ligands had permanent positive and negative charges (pK_a of sulfonic acid is ~1.5, so it can be treated as always fully deprotonated over the pH range of 3−12 in which the NPs are stable).
(15) Thorek, D. L. J.; Tsourkas, A. *Biomaterials* **2008**, *29*, 3583.
(16) Slowing, I.; Trewyn, B. G.; Lin, V. S. Y. *J. Am. Chem. Soc.* **2006**, *128*, 14792.
(17) When discussing on-particle mixed monolayers, one should consider potential phase separation, as in the systems described by the Stellacci and Glotzer groups (see: Jackson, A. M.; Myerson, J. W.; Stellacci, F. *Nat. Mater.* **2004**, *3*, 330; Singh, C.; Ghorai, P. K.; Horsch, M. A.; Jackson, A. M.; Larson, R. G.; Stellacci, F.; Glotzer, S. C. *Phys. Rev. Lett.* **2007**, *99*, 226106). In our case, however, phase separation of the SAM into all-MUA and all-TMA domains is highly unlikely, as it would lead to the colocalization of like-charged moieties. Such a scenario would be energetically unfavorable because of electrostatic repulsions.
(18) Walker, D. A.; Kowalczyk, B.; de la Cruz, M. O.; Grzybowski, B. A. *Nanoscale* **2011**, *3*, 1316.
(19) Browne, K. P.; Grzybowski, B. A. *Langmuir* **2011**, *27*, 1246.
(20) Ulman, A. *Chem. Rev.* **1996**, *96*, 1533.
(21) Williams, Y.; Sukhanova, A.; Nowostawska, M.; Davies, A. M.; Mitchell, S.; Oleinikov, V.; Gun'ko, Y.; Nabiev, I.; Kelleher, D.; Volkov, Y. *Small* **2009**, *5*, 2581.
(22) Cytotoxicity was observed at higher concentrations of NPs. This is summarized in Figure S8 for 5−500 nM concentrations of α_{surf} = 1.2 MC NPs and for the same concentrations of fully positively charged NPs whose cytotoxicity was investigated previously (see: Leroueil, P. R.; Berry, S. A.; Duthie, K.; Han, G.; Rotello, V. M.; McNerny, D. Q.; Baker, J. R.; Orr, B. G.; Holl, M. M. B. *Nano Lett.* **2008**, *8*, 420; Frohlich, E. *Int. J. Nanomed.* **2012**, *7*, 5577). The images in Figure S8 and the ICP uptake data in Table S1 show that although the all-TMA NPs were uptaken ~3 times more efficiently than the MC NPs, they were also significantly more cytotoxic (e.g., 90% of cells died in the presence of 250 nM all-TMA NPs vs only 4% in the presence of 250 nM MC NPs).
(23) Giljohann, D. A.; Seferos, D. S.; Patel, P. C.; Millstone, J. E.; Rosi, N. L.; Mirkin, C. A. *Nano Lett.* **2007**, *7*, 3818.
(24) Albanese, A.; Tang, P. S.; Chan, W. C. W. *Annu. Rev. Biomed. Eng.* **2012**, *14*, 1.
(25) Chithrani, B. D.; Chan, W. C. W. *Nano Lett.* **2007**, *7*, 1542.
(26) Gratton, S. E. A.; Ropp, P. A.; Pohlhaus, P. D.; Luft, J. C.; Madden, V. J.; Napier, M. E.; DeSimone, J. M. *Proc. Natl. Acad. Sci. U.S.A.* **2008**, *105*, 11613.
(27) Gao, H. J.; Shi, W. D.; Freund, L. B. *Proc. Natl. Acad. Sci. U.S.A.* **2005**, *102*, 9469.
(28) Chithrani, B. D.; Ghazani, A. A.; Chan, W. C. W. *Nano Lett.* **2006**, *6*, 662.
(29) Cedervall, T.; Lynch, I.; Lindman, S.; Berggard, T.; Thulin, E.; Nilsson, H.; Dawson, K. A.; Linse, S. *Proc. Natl. Acad. Sci. U.S.A.* **2007**, *104*, 2050.
(30) Choi, H. S.; Liu, W.; Misra, P.; Tanaka, E.; Zimmer, J. P.; Ipe, B. I.; Bawendi, M. G.; Frangioni, J. V. *Nat. Biotechnol.* **2007**, *25*, 1165.
(31) Fleige, E.; Quadir, M. A.; Haag, R. *Adv. Drug Delivery Rev.* **2012**, *64*, 866.
(32) Gerweck, L. E.; Seetharaman, K. *Cancer Res.* **1996**, *56*, 1194.
(33) Lehner, R.; Wang, X. Y.; Wolf, M.; Hunziker, P. *J. Controlled Release* **2012**, *161*, 307.